Research Paper

Journal of Engineering and Technological Sciences

Rapid Flood Mapping Using Statistical Sampling Threshold Based on Sentinel-1 Imagery in the Barito Watershed, South Kalimantan Province, Indonesia

Muhammad Priyatna[1,2*], Muhammad Rokhis Khomarudin[1], Sastra Kusuma Wijaya[2], Fajar Yulianto[1], Gatot Nugroho[1], Pingkan Mayestika Afgatiani[1,3], Anisa Rarasati[1] & Muhammad Arfin Hussein[4]

[1]Research Center for Remote Sensing Technology, Research Organization for Aeronautics and Space, National Research and Innovation Agency, East Jakarta, 13710, Indonesia
[2]Physics Department, Faculty of Mathematics and Natural Sciences, University of Indonesia, Depok, 16424, Indonesia
[3]Faculty of Science, Graduate School of Science and Engineering, University of the Ryukyus, Okinawa, Japan
[4]Instrumentation Electronics Study Program, Indonesian Nuclear Technology Polytechnic, Yogyakarta, Indonesia

*Corresponding author: muha054@brin.go.id

Abstract

Flood disasters occur frequently in Indonesia and can cause property damage and even death. This research aimed to provide rapid flood mapping based on remote sensing data by using a cloud platform. In this study, the Google Earth Engine cloud platform was used to quickly detect major floods in the Barito watershed in South Kalimantan province, Indonesia. The data used in this study were Sentinel-1 images before and after the flood event, and surface reflectance of Sentinel-2 images available on the Google Earth Engine platform. Flooding is detected using the threshold method. In this study, we determined the threshold using the Otsu method and statistical sampling thresholds (SST). Four SST scenarios were used in this study, combining the mean and standard deviation of the difference backscatter of Sentinel-1 images. The results of this study showed that the second SST scenario could classify floods with the highest accuracy of 73.2%. The inundation area determined by this method was 4,504.33 km^2. The first, third and fourth SST scenarios and the Otsu method could reduce the flood load with an overall accuracy of 48.37%, 43.79%, 55.5% and 68.63%, respectively. The SST scenario is considered to be a reasonably good method for rapid flood detection using Sentinel-1 satellite imagery. This rapid detection method can be applied to other areas to detect flooding. This information can be quickly produced to help stakeholders determine appropriate flood management strategies.

Keywords: *flood; Barito watershed; Sentinel-1; statistical sampling; threshold.*

Introduction

Flooding can be defined as the process of water overflowing land areas and the tides associated with this overflow [1,2]. Floods are often considered disasters when people are affected by their impacts [3]. Flood disasters are not uncommon in Indonesia [4-6] and occur more frequently in the western regions of the country due to higher rainfall [7].

Flood disasters can cause property damage and disruption of community activities [8] and often result in fatalities [9]. In addition to the initial damage, floods can also cause numerous post-event problems. Disease outbreaks are an example of a secondary disaster that can be triggered by flooding [10]. Flood disasters usually bring the economic life of the affected communities to a standstill, necessitating the provision of assistance to those affected.

ISSN: 2337-5779
DOI: 10.5614/j.eng.technol.sci.2023.55.1.10

DOI: 10.5614/j.eng.technol.sci.2023.55.1.10

Information on the location of flood events is needed to facilitate the distribution of relief supplies and the management of flood disasters. Large floods, such as those in Indonesia's South Kalimantan province, have covered wide areas and damaged some settlement, forest, plantation, and agricultural areas. Therefore, resources must be available to effectively map floodplains. The problems associated with this mapping can be solved using remote sensing technologies, which have the advantage of covering larger areas than conventional methods and always providing up-to-date data, which is part of the role of remote sensing data and information in the disaster management cycle [11-13]. Remote sensing data can support modeling of flood-prone areas [14]. The frequency ratio is an example of a methodological approach to modeling the degree of flood hazard based on remote sensing data [15,16]. In addition, remote sensing data have the potential to be used as input for flood detection.

Remote sensing technologies have been used to detect areas of water in the form of transient puddles that occur during floods. Images in the green band and NIR band are used to detect water bodies using the normalized difference water index (NDWI) [17,18]. Since the green band can increase the reflectance of water bodies and the NIR band can decrease the reflectance, these two bands are used. On the west coast of West Lombok, the NDWI is used to identify water bodies. If the image used is cloud-free, optical imaging can be used to identify bodies of water; however, if there is heavy cloud cover, flooding is more likely. As a result, optical imagery loses clarity, and radar imagery may be more effective [19].

The advantage of radar satellite imagery is that it is unaffected by cloud cover [20] and is therefore suitable for detecting water bodies [21,22]. Although radar imagery can detect water bodies well, radar satellite imagery, which is acquired only once, cannot determine the difference between floods and pre-existing water bodies such as lakes. Therefore, in this study, we attempted to use multi-temporal Sentinel-1 radar satellite imagery to distinguish receiving waters from flooded areas. Several studies have used a specific threshold to detect flooding from radar imagery [23-26]. The objective of this study was to determine the ability of certain statistical thresholds and the Otsu method to detect flooded areas in the Barito watershed in South Kalimantan province, Indonesia. The use of a threshold on Sentinel- 1 data enables rapid detection of floodplains that can be used for rapid disaster management. While some research has been conducted using SAR imagery, it used expensive data such as TerraSAR X [27]. The advantage of using Sentinel-1 data is that it is available for free on a cloud platform.

Materials and Methods

Location

The Barito watershed is located in the administrative area of South Kalimantan province (Figure 1). Geographically, the Barito watershed is located at 114°20' to 115°52' and 1°0' to -3°44'. The Barito catchment is one of the most important watersheds in Borneo. The provinces of South Kalimantan and Central Kalimantan are both located in the headwaters of this watershed. In January 2021, the Barito watershed experienced unusually heavy rains that caused flooding in several locations. The flood event in the Barito watershed, particularly in the province of South Kalimantan, was an exceptional flood event. It was the largest flood in the last 50 years. The flood also affected 5,000 inhabitants [28]. Therefore, this place can be used as learning material for research related to flood disasters.

Data

Sentinel-1 multi-temporal imagery was employed in this study. Sentinel-1 image mosaic for July 2020 was used for the 'before flood' imaging (Figure 2a), while the January 2021 post-flood imaging was based on the Sentinel-1 picture mosaic (Figure 2b). The Google Earth Engine (GEE) platform provided the information used. VV polarization was used to detect flood areas, making it simpler to detect flooding in regions where there is vegetation, according to a study conducted in Pakistan [29]. Because of the effect of multiple reflections generated by water surfaces and vegetation, VV polarization is used in flood monitoring, and the majority of backscattering exhibits stable polarization [30].

Sample data from flood locations obtained from the Indonesian National Disaster Management Agency (BNPB) and the PetaBencana.id portal were used in threshold calculations and accuracy checks (Figure 3). The sampling points were located across the Barito watershed from the upper to the lower reaches. There were 178 sample points consisting of 65 non-flood sample points and 113 flood sample points. The limited number of sample points for flood locations, which were only 113 points, made the authors use 25 samples as training data for the statistical sample threshold and 88 other flood points as validation tests. A small number of samples intended to test if there are limited field data conditions as training due to flooding and whether rapid detection of flood inundation using this approach can still produce good results.

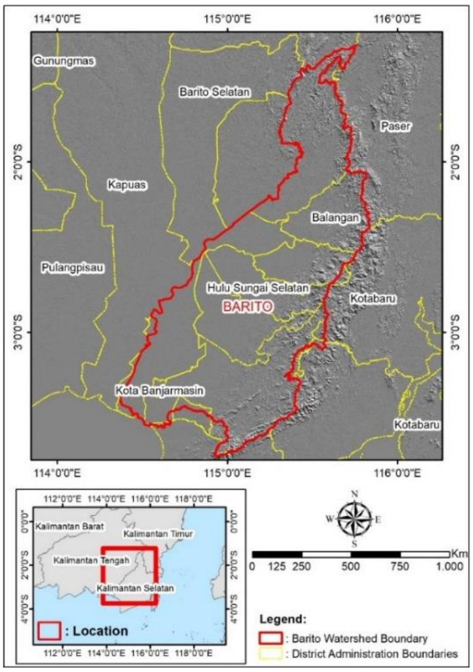

Figure 1 Research location in the Barito watershed in South Kalimantan.

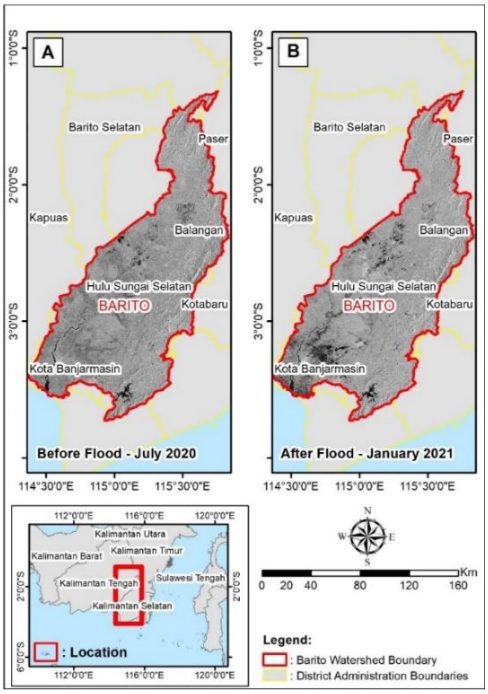

Figure 2 Images used in this study. (Source: GEE).

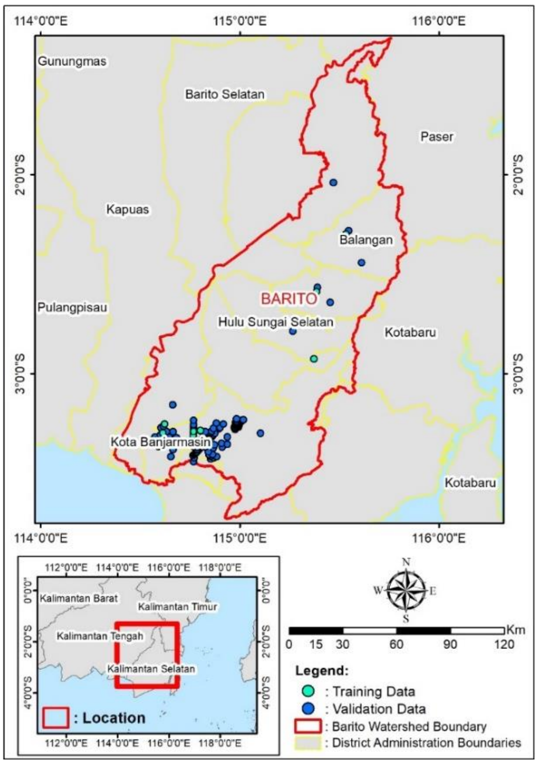

Figure 3 Samples of flood data. (Sources: BNPB and PetaBencana.id)

Method

The fastest approach for binary classification of a picture is the threshold method. Choice of the correct threshold is a key aspect in this procedure since it affects the classification outcomes [31]. Several methods can be applied to determine the threshold. In this study, we will use statistical sample thresholds and the Otsu method to determine the detection threshold for flood inundation in the Barito watershed, South Kalimantan. In general, the flood inundation detection method in the Barito watershed, South Kalimantan Province, consists of (1) pre-processing, (2) processing, and (3) assessment, as shown in Figure 4.

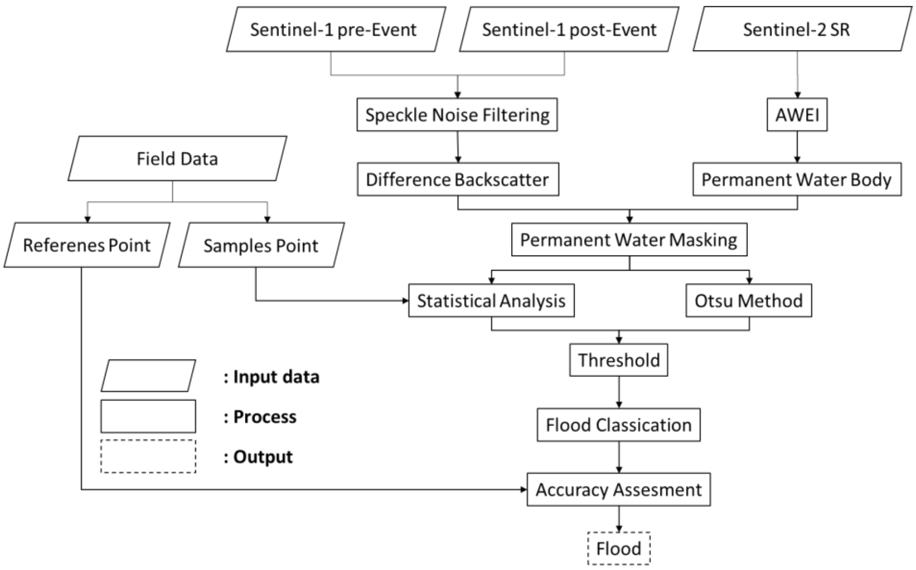

Figure 4 Rapid flood mapping process.

1. **Pre-processing:** The Sentinel-1 VV imagery was used to map flood inundation and GEE was used to process the data. The pre-processing stage was carried out to prepare the data to be ready to be used as input for determining the threshold and detection of flood inundation. This stage consisted of several steps, including area focusing, Sentinel-1 image speckle noise correction, determination of backscattering differences, detection of permanent water bodies from Sentinel-2 SR images, and preparation of flood samples. Deductions were made on the area of interest, specifically the Barito watershed boundary in South Kalimantan Province, Indonesia, to speed up processing time. To remove the effect of speckle noise, a 3 x 3 median filter was used, chosen because it produces a superior signal-to-noise ratio [23].
2. Detection of permanent water bodies was carried out from the 2020 mosaic Sentinel-2 images using the automatic water extraction index (AWEI). Permanent water bodies are pixels with a value greater than -0.232 [32]. This permanent water body is used as a mask so that the permanent water body can be removed from the Sentinel-1 image. This process is done to minimize errors in flood detection results. Furthermore, ordinary mathematical processes were used to calculate the difference between the mixed values. The difference in scattering values was calculated by subtracting the post-flood data from the data collected before the flood.
3. **Processing**: Determination of the threshold for detecting flood inundation in this study was conducted using two methods. The first method was performed by using a statistical sample threshold. The second method used to obtain flood threshold values is the Otsu method.
4. The Otsu approach uses a criterion measure to assess the variance between threshold classes before applying it to the image to create a flood map with wet and dry pixels [32]. The Otsu technique is a method of classification that uses a global threshold to discriminate between groups based on data from a normal distribution [23]. The technique divides the data into two groups based on the grey level [33], the first class having low grey level value and the second having high grey level value. Calculation of variance determines the grey level. Flood maps have been made using this technology for a significant time. Eq. (1) shows how to calculate the Otsu threshold [30]:

$$\left\{\begin{matrix} \delta^2 = P_{nw}(M_{nw} - M)^2 + P_w(M_w - M)^2 \\ M = P_{nw}M_{nw} + P_wM_w \\ P_{nw} + P_w = 1 \\ Th_{Otsu} = Arg \max_{x \le Th_{Otsu} \le y} (\delta^2) \end{matrix}\right\} \tag{1}$$

In Eq. (1), δ^2 is the variance between classes of water bodies and non-water bodies; M_{nw} and M_w are the average pixels of non-water bodies and water bodies; P_{nw} and P_w are the probabilities of pixels belonging to the non-water-body or the water-body class; M is the average of the entire image.

The other threshold method used in this research was the statistical sample threshold. The statistical sample threshold is a threshold determination method that is carried out by calculating the average value and standard deviation of the difference between Sentinel-1 backscattering images before and after flooding. The goal of this strategy is to simplify classification by combining threshold- and sample-based guided classification with limited samples. A mixture of statistical values is used to establish the threshold value. The average value and standard deviation were obtained from the sample points where the flood occurred. This study used four SST calculation scenarios, as indicated by Eqs. (2) to (5). Threshold Th is calculated using the following simple mathematical operations:

$$Th_1 = \bar{x} - \sigma \tag{2}$$

$$Th_2 = \bar{x} + \sigma \tag{3}$$

$$Th_3 = \bar{x} - 1.5\sigma \tag{4}$$

$$Th_4 = \bar{x} + 1.5\,\sigma \tag{5}$$

where $\bar{x}$ is the sample mean and σ is the sample standard deviation.

DOI: 10.5614/j.eng.technol.sci.2023.55.1.10

Results and Discussion

Flood Mapping

Flood Detection

The distribution of pixels representing wet and dry areas are visible in the threshold results. Flooded locations are those that are flooded with water; the southern half of the Barito watershed is where flood inundation is most noticeable (Figure 5). In the south, the downstream portion of the Barito watershed has a rather flat topography. Cities with dense residential populations can be found in this area and as a result, if flooding occurs, its impact will be large. Each threshold has the potential to detect floods, as can be seen from the maps. However, statistical thresholds 2 and 4 detected significantly more flooding than the other thresholds, as demonstrated by the dominant blue areas. It is possible to determine the flood area based on these data. The Otsu detected floods with an area of 1,096.28 km^2 utilizing flood detection. Flooding can also be detected using the proposed sample threshold statistical method. Using Eq. (2), the flood inundation area detected using statistical threshold 1 was 269.55 km^2. Flood areas of 4,504.01 km^2, 134.33 km^2 and 16,444.88 km^2 were detected using statistical thresholds 2, 3, and 4, respectively.

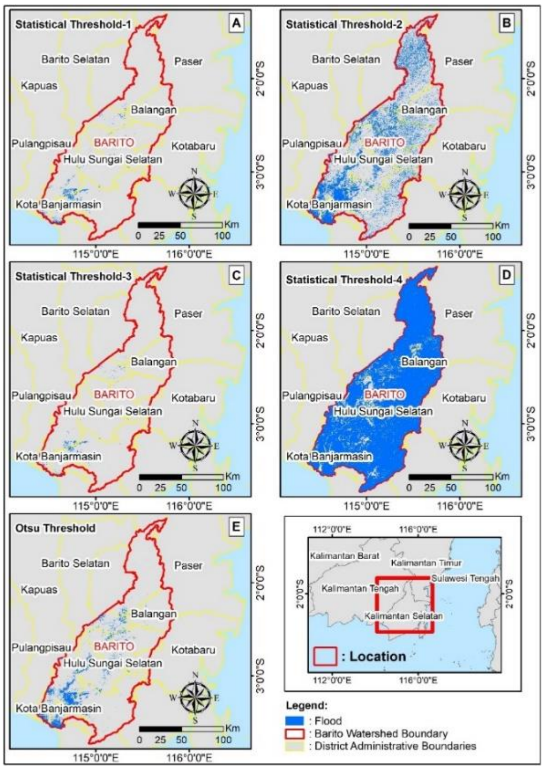

Figure 5 Barito watershed flood detection results using (A) statistical threshold 1, (B) statistical threshold 2, (C) statistical threshold 3, (D) statistical threshold 4, and (E) the Otsu threshold.

The Otsu threshold approach can accurately and clearly detect floods and produces acceptable results. In locations with a rather flat slope, floods are recorded (Figure 6). Meanwhile, the flooding observed using the statistical sample threshold technique appears to be exaggerated for statistical thresholds 1 and 2 and is more likely to be underestimated for statistical threshold 3. Even in places with a rather steep slope, both systems detect flooding. With results that are close to the Otsu threshold, statistical threshold 1 can detect flooding.

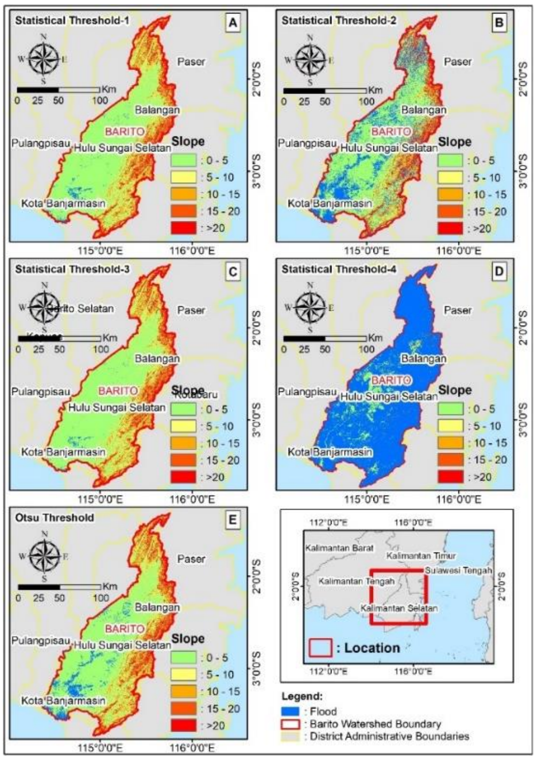

Figure 6 Flood inundation overlay with slope data.

Accuracy Assessment

A total of 153 flood location locations were used in the accuracy test. The test point locations were picked at random. A confusion matrix approach was used to conduct the accuracy testing, providing an overall accuracy index, chosen because it is a typical approach used for describing classification accuracy [13]. According to the accuracy test findings, threshold 2 had the highest accuracy, at 73.2%, while threshold 3, with a precision of 43.79%, had the lowest accuracy. The accuracy test results are summarized in Table 1.

Table 1 Accuracy test result.

Methods	Omission error		Commission error		Overall accuracy
	Flood	Not flood	Flood	Not flood	
Th1	9.09	54.93	88.64	68.99	48.37
Th2	14.93	36.05	35.23	11.18	73.20
Th3	25.00	57.05	96.59	0.00	43.79
Th4	42.96	63.64	7.95	4.72	55.56
Otsu	6.52	42.06	51.14	4.62	68.63

Statistical Sample Threshold Performance

Floods in open locations are easily detectable. However, in highly inhabited areas floods cannot be identified clearly using either the statistical sample threshold or the Otsu threshold approach. This finding can be attributed to a variety of factors. One of the causes is that the spatial resolution employed is limited. Sentinel-1 images with a resolution of 10 m will be more dominant in receiving backscatter from the roofs of buildings in places that are particularly densely populated. Backscatter is caused by flood conditions that do not submerge the entire roof of the building, but which are captured by sensors as reflections from the roofs. In addition, flooding in residential areas can cause radar waves to experience double-bounce backscattering. Double-bounce backscattering causes the backscattering value to be higher. As a result, the backscatter difference value becomes positive and is not identified as a flood area [32].

Furthermore, because water that has retreated does not indicate tiny variations from the before-flood images, the time interval between the flood event and the final image used can alter the flood classification. The

DOI: 10.5614/j.eng.technol.sci.2023.55.1.10

backscattering of water and non-water objects is significantly distinct, hence, these images can be used to discern between the two [31].

Because the backscatter during/after the flood is smaller than before the flood, the calculation used of the difference in backscatter value of the flood point after and before the event will generate a negative number. This condition applies to relatively open areas such as agricultural land and bare soil. This phenomenon is among the results of [32], which shows that the difference between Sentinel-1 backscattering before and after flooding in relatively open areas is negative. This is because bodies of water will cover objects other than bodies of water. In contrast to an item that was previously a body of water, the backscatter value after and before the flood will be nearly identical. This could reveal the difference between a permanent body of water and a flood inundation. The VV polarization backscattering of aquatic bodies ranges between -22.4 dB and -12.9 dB. For non-water bodies, the backscattering of VV polarization ranges between -10.8 dB and -1 dB [31]. As a result, the backscatter difference has a negative value.

The statistical calculation of the sample revealed an average backscattering difference of 0.94 dB with a standard deviation of 1.5 dB. Flooding is determined to have a backscattering differential value smaller than the threshold. As a result, if the value of $\bar{x}$ is dropped by σ or 1.5σ, the threshold value is smaller, and there are locations with values around $\bar{x}$ that are not detected as floods, resulting in underestimates for statistical threshold 1 and statistical threshold 3. If the threshold value is multiplied by a number that is too great, non-flood sites will be recognized as flooding. As a result, statistical threshold 4 produces overestimates. With a limited number of samples, the statistical sample threshold method for scenario 2 is sufficient to provide results with reasonably good accuracy, i.e., above 70%. Thus, this method has the potential to be applied in rapid flood mapping where sample availability is challenging to obtain.

Meanwhile, adding σ will cause numerous flood readings acquired between $\bar{x}$ and $\bar{x} + \sigma$ to be detected as flooding, enhancing accuracy when compared to using $\bar{x}$ as threshold. The precision of this strategy is better when it comes to locating flood events on flat terrain. However, such calculations will still have certain limitations in places with a fairly steep slope, causing the results to be overstated. In order to improve the method's capabilities, more post-classification work is required. In this, the use of DEM data as a filter has the potential to be useful.

The use of statistical sample thresholds, particularly scenario 2, has the potential to be further developed, since J. Liang and D. Liu [24] found that local thresholds have the potential to be more accurate than global thresholds. Various scenarios that refer to land cover types may be further developed to overcome the problem of double-bounce backscatter flood inundation in urban areas.

The method of mapping floods based on historical remote sensing data is feasible. Furthermore, the integration of the results of the analysis of the mapping of flood inundation historically with flood modeling is interesting to be developed. At present, several flood modeling methods have been developed, such as the Hydraulic Model [33], the Flood Risk Map Model [34], and the Potential Flood Model [35]. These models can be integrated with the flooding inundation mapping based on the satellite image of remote sensing. The results of the analysis are expected to provide an overview related to the phenomenon of flooding to the Indonesian government in developing flood control policies and flood management solutions as the government of Indonesia did in formulating solutions for handling floods in Semarang, Central Java, Indonesia [36].

Conclusions

A statistical sampling threshold can be used to detect flood episodes in South Kalimantan Province of Indonesia. The statistical sample threshold showed its potential for rapid flood mapping using Sentinel-2 imagery. The second statistical sample threshold scenario could produce good results with an overall accuracy value of 73.2%. In this study, the Otsu threshold did not provide the best accuracy. In open areas without structures, the statistical threshold 2 data and methods employed could detect flood areas fairly well. Although the accuracy test results showed good enough results for fast mapping, this method needs to be further developed, for example by considering the existing land cover types.

Acknowledgments

The authors are grateful to the USGS, ESA, KLHK, BNPB, PetaBencana.id, and GEE for providing free data for this research.

Funding

This research was supported by PUTI NKB-617//UN2.RST/HKP.05.00/2020 from University of Indonesia.

References

[1] Patel, D.P. & Srivastava, P.K., *Flood Hazards Mitigation Analysis Using Remote Sensing And GIS: Correspondence with Town Planning Scheme*, Water Resources Management, **27**, pp. 2353-2368, 2013.

[2] Rizkiah, R., Poli, H. & Supardjo, H., *Analysis of Factors Causing Floods in Tikala District, Manado City*, Journal SPASIAL: Perencanaan Wilayah dan Kota, 1(1), pp. 105-112, 2015.

[3] Savitri, E. & Pramono, I.B., *Upper Cimanuk Flood Analysis of 2016,* Jurnal Penelitian Pengelolaan Daerah Aliran Sungai, **1**(2), pp. 97–110, 2017.

[4] Hamdani, H., Permana, S. & Susetyaningsih, S., *Analysis of Flood-Prone Areas Using Geographic Information System Applications (Case Study of Bangka Island),* Jurnal Konstruksi Sekolah Tinggi Teknologi Garut, **12**(1), pp.1-13, 2014. (Text in Indonesian)

[5] Yulianto, F., Suwarsono, Sulma, S. & Khomarudin, M.R., *Observing the Inundated Area Using Landsat-8 Multitemporal Images and Determination of Flood-Prone Area in Bandung Basin*, International Journal Remote Sensing and Earth Sciences, **15**(2), pp. 131-140, 2018.

[6] Priya, M.G. & Divya, N., *Measurement to Management: Study of Remote Sensing Techniques for Flood Disaster Management*, Journal of Remote Sensing and GIS, **10**(1), pp.40-57, 2019.

[7] Putri, Y.P., Barlian, E., Dewata, I. & Tanto, T.A., *Policy Direction on Flash Floods Disaster Mitigation in Kuranji Watershed, Padang City*, Majalah Ilmiah Globe, **20**(2), pp. 87-98, 2018.

[8] Prastica, R.M.S., Maitri, C., Nugroho, P.C. & Hermawan, A*., Flood Analysis and River Transportation Design Planning in Bojonegoro City*, Media Komunikasi Teknik Sipil, **23**(2), pp. 91-101, 2017.

[9] Findayani. A., *Community Readiness in Flood Management in the City of Semarang*, Jurnal Geografi, **12**(1), pp. 102-114, 2015.

[10] Maulana, E. & Wulan, T.R., *Multi-hazard Mapping of Southern Malang Regency Using a Landscape Approach*, National Symposium of Geoinformation Science IV 2015, pp. 526-534, 2015. (Text in Indonesian)

[11] Westen, C.V., *Remote Sensing for Natural Disaster Management*, International Archives of Photogrammetry and Remote Sensing, **XXXIII**(B7), pp. 237-245, 2000.

[12] Kader, M.A. & Jahan, I., *A Review of the Application of Remote Sensing Technologies in Earthquake Disaster Management: Potentialities and Challenges*, International Conference on Disaster Risk Management, 2019.

[13] Kaku, K., *Satellite Remote Sensing for Disaster Management Support: A Holistic and Staged Approach Based on Case Studies in Sentinel Asia*, International Journal of Disaster Risk Reduction, **33**, pp. 417-432, 2019.

[14] Sarkar, D. & Mondal, P., *Flood Vulnerability Mapping Using Frequency Ratio (FR) Model: A Case Study on Kulik River Basin, Indo-Bangladesh Barind Region*, Applied Water Science, **10**(17), 2020.

[15] Saha, S., Sarkar, D. & Mondal, P., *Efficiency Exploration of Frequency Ratio, Entropy and Weights of Evidence-Information Value Models in Flood Vulnerability Assessment: A Study of Raiganj Subdivision*, Eastern India, Stochastic Environmental Research and Risk Assessment, **36**, pp. 1721-1742, 2021.

[16] Sarkar, D., Saha, S. & Mondal, P., *GIS-Based Frequency Ratio and Shannon's Entropy Techniques for Flood Vulnerability Assessment in Patna District*, Central Bihar, India, Int. J. Environ. Sci. Technol., **19**, pp. 8911-8932, 2021.

[17] Kusumawardani, K.P., Cahya, Z.I., Ananto, W.H.G. & Asri, G.H.M., *Mapping and Analysis of Shoreline Change In West Coast Lombok Barat Using Normalized Difference Water Index on Landsat Imagery*, Seminar Nasional Geomatika 2018, pp. 911-918, 2018.

DOI: 10.5614/j.eng.technol.sci.2023.55.1.10

[18] Soltanian, F.K., Abbasi, M. & Bakhtyari, H.R.R., *Flood Monitoring Using NDWI And MNDWI Spectral Indices: A Case Study of Aghqala Flood–2019, Golestan Province, Iran*, International Archives of the Photogrammetry, Remote Sensing and Spatial Information Sciences, XLII-4(W18), GeoSpatial Conference 2019 – Joint Conferences of SMPR and GI Research, pp. 605-607, 2019.

[19] Nasirzadehdizaji, R., Akyuz, D.E. & Cakir, Z., *Flood Mapping and Permanent Water Bodies Change Detection Using Sentinel SAR Data*, The International Archives of the Photogrammetry, Remote Sensing and Spatial Information Sciences, XLII-4(W18), GeoSpatial Conference 2019 – Joint Conferences of SMPR and GI Research, pp. 797-801, 2019.

[20] Sunuprapto, H. & Hussin, Y.A., *A Comparison between Optical and Radar Satellite Images in Detecting Burnt Tropical Forest In South Sumatra, Indonesia*, International Archives of Photogrammetry and Remote Sensing, XXXIII(B7), pp. 580-587, 2000.

[21] Anusha, N. & Bharathi, B., *Flood Detection and Flood Mapping Using Multi-Temporal Synthetic Aperture Radar and Optical Data*, The Egyptian Journal of Remote Sensing and Space Science, **23**(2), pp. 207-219, 2019.

[22] Waru, A.T., Bayanuddin, A.A., Nugroho, F.S. & Rukminasari, N., *Temporal Analysis of Mangrove Forest Changes Using Sentinel-2 Satellite Imagery: Case Study in Tanakeke Island, Takalar District*, Geomatics National Seminar 2020: Geospatial Information for Innovation to Accelerate Sustainable Development, pp. 777–786, 2020.

[23] Cao, H., Zhang, H., Wang, C. & Zhang, B., *Operational Flood Detection Using Sentinel-1 SAR Data Over Large Areas*, Water, **11**(4), 786, 2019.

[24] Liang, J. & Liu, D., *A Local Thresholding Approach to Flood Water Delineation Using Sentinel-1 SAR Imagery*, ISPRS J. Photogramm, **159**, pp. 53-62, 2019.

[25] Berezowski, T., Bielinski, T. & Osowicki, J., *Flooding Extent Mapping for Synthetic Aperture Radar Time Series Using River Gauge Observations*, IEEE Journal of Selected Topics in Applied Earth Observations and Remote Sensing, **13**, pp. 2626-2638, 2020.

[26] Tiwari, V., Kumar, V., Matin, M.A., Thapa, A., Ellenburg, W.L., Gupta, N. & Thapa, S., *Flood Inundation Mapping– Kerala 2018; Harnessing the Power of SAR, Automatic Threshold Detection Method and Google Earth Engine*, PLoS ONE, **15**(8), e0237324, 2020.

[27] Martinis, S., Kersten, J. & Twele, A., *A Fully Automated Terrasar-X Based Flood Service*, ISPRS Journal of Photogrammetry and Remote Sensing, **104**, pp. 203-212, 2014.

[28] Puspitarini, R.C., *Perspectives on South Kalimantan Floods in 2021*, JISIP, **1**(1), pp. 1-14, 2021.

[29] Zhang, M., Chen, F., Liang, D., Tian, B. & Yang, A., *Use of Sentinel-1 GRD SAR Images to Delineate Flood Extent in Pakistan*, Sustainability, **12**(14), pp. 1-19, 2020.

[30] Zhang, M., Li, Z., Tian, B., Zhou, J. & Tang, P., *The Backscattering Characteristics of Wetland Vegetation and Water-Level Changes Detection Using Multi-Mode SAR: A Case Study*, International Journal of Applied Earth Observation and Geoinformation, **45**, pp. 1–13, 2016.

[31] Uddin, K., Matin, M.A. & Meyer, F.J., *Operational Flood Mapping Using Multi-Temporal Sentinel-1 SAR Images: A Case Study from Bangladesh*, Remote Sensing, **11**(13), pp. 1-19, 2019.

[32] Papila, I., Alganci, U. & Sertel, E., *Sentinel-1 Based Flood Mapping Using Interferometric Coherence and Intensity Change Detection Approach*, The International Archives of the Photogrammetry, Remote Sensing and Spatial Information Sciences, XLIII-B3-2020, XXIV ISPRS Congress (2020 edition), 2020.

[33] Wurjanto, A., Tarigan, T.A. & Mukhti, J.A., *Flood Routing Analysis of the Way Seputih River, Central Lampung, Indonesia*, International Journal of GEOMATE, **17**(63), pp. 307-314, 2019.

[34] Formánek, A., Silasari, R., Kusuma, M.S.B. & Kardhana, H., *Two-Dimensional Model of Ciliwung River Flood in DKI Jakarta for Development of the Regional Flood Index Map*, J. Eng. Technol. Sci., **45**(3), pp. 307-325, 2013.

[35] Susandi, A., Tamamadin, M., Pratama, A., Faisal, I., Wijaya, A.R., Pratama, A.F., Pandini, O.P. & Widiawan, D.A., *Development of Hydro-Meteorological Hazard Early Warning System in Indonesia*, J. Eng. Technol. Sci., **50**(4), pp. 461-478, 2018.

[36] Wurjanto, A., Mukhti, J.A. & Wirasti, H.D., *Study of Pump and Retention Basin Requirement for Semarang-Demak Coastal Dike Plan, Central Java*, International Journal of GEOMATE, **15**(47), pp. 66-73, 2018.

Manuscript Received: 5 October 2022
1st Revised Manuscript Received: 30 December 2023
2nd Revised Manuscript Received : 27 February 2023
Accepted Manuscript: 28 February 2023